Vol. 46, No. 2 (2024) 260-269, DOI: 10.24874/ti.1555.09.23.11

Tribology in Industry

www.tribology.rs

RESEARCH

# Evaluation of Wear Model Equations Through Analysis of Experimental Wear Data of Materials from Literature

Shivasharanappa V. Gubbewad[a] and Amaresh Raichur[b,*]

[a]*Department of Automobile Engineering P. D.A. College of Engineering Kalaburagi. Karnataka India,*
[b]*Department of Ceramic and Cement Technology P. D.A. College of Engineering Kalaburagi. Karnataka India.*

Keywords:

*Wear*
*Wear equations*
*Pin-on-disc*
*Wear rate*
*Wear volume*

* Corresponding author:

*Amaresh Raichur*
*E-mail: amareshr@pdaengg.com*

*Received: 21 September 2023*
*Revised: 12 October 2023*
*Accepted: 15 November 2023*

A B S T R A C T

*Understanding the correlation between material characteristics and wear behavior helps in the development and manufacturing of high-quality materials for components subjected to wear, like brake pads, bearings etc.*

*The majority of published research papers present experimental data from pin-on-disc experiments in which wear volume loss is measured using wear rate and sliding distance. However, in many publications pin on disc experimental data is interpreted by statistical methods like Taguchi method to understand the effect of material characteristics on wear behavior. This method indirectly correlates wear behavior to material parameters like hardness, modulus of elasticity and toughness of the material. However, many mathematical models are proposed in literature to directly relate material characteristics to wear behavior.*

*However, there are gaps in published literature in interpretation of experimental data with mathematical model equations. The mathematical models like Archard model, Evans and Wilshaw model, Kato model etc proposed in literature are defined to link material characteristics like modulus of elasticity, hardness, toughness etc to wear behavior.*

*In this study, it is proposed a methodology to interpret the pin on disc experimental wear data by fitting an analytical model to understand effect of material characteristics on wear behavior of materials.*



## 1. INTRODUCTION

Analysis of data from wear tests on engineering materials and composites will give an insight into their development and applications for high-quality materials components subjected to wear, like brake pads, bearings, aerospace, turbine blades, nuclear reactors, fuel rods, sealant, etc.

The amount of wear depends on a number of factors, both on material characteristics and testing conditions that affect the wear performance of materials.

Material characteristics include hardness, toughness, strength, elastic modulus, grain sizes, reinforced phases, etc. [1,2]

Factors affecting wear due to testing conditions on Pin-on Disc instrument includes, applied load, disc-hardness, temperature, sliding speed, sliding distance, environment, etc. [1–3]. Experimental results of Pin-on Disc can be used to evaluate the wear performance of the material. In literature, it is observed that experimental wear data is analyzed by the Taguchi method to study the effect of material property on wear behavior. It is often observed that experimental wear data is analyzed by the Taguchi method to study the effect of constituents and characteristics of materials on wear performance [4–6]. Interpretation of pin-on-disc wear data is carried out by Taguchi method for design of experiments to investigate how different parameters affect the mean and variance of a process performance characteristic on wear. However, the main drawback of Taguchi method for wear data analysis is that the results obtained are compared with relative effect of each constituent phase on wear performance.

There is a gap in the literature when it comes to the examination and verification of analytical models that are suggested using experimental data. In this work, X-Y extract software is used to measure published experimental wear data on pin-on-discs from several published research articles. To account for the physical characteristics of the materials that influence wear behaviour, the data is transformed into the necessary format, i.e., load v/s volume loss (wear volume loss), and then interpreted by fitting linear wear equations [7] using linear trend line and power law wear equations [7,8] using power trend line.

## 2. LITERATURE REVIEW

Wear behavior related to the material properties such as strength, hardness, toughness and microstructure [1,2]. In literature Design of experiments was used to investigate how different parameters affect the mean, variance, and S/N (signal to noise ratio) [4,6]. The role of constituents on performance of wear behavior of composites was studied by analysis of experimental wear data was carried out by keeping one constituent constant and varying others. It is often observed that experiment wear data was analyzed by Taguchi method to study the effect of constituents on wear performance of materials when subjected to a pin-on disc condition [4–6].

Bortoleto et al. [1] compared the experimental results on materials, AISI4140 steel pins and AISIH13 steel discs in the pin on disc trials, with estimated wear loss obtained from numerical analysis based on the linear Archard's wear law and finite element modeling (FEM).

Bortoleto et al. [1] observed that despite the use of a global wear coefficient derived from experimental data in numerical simulations, the numerical method was unable to accurately replicate experimental data because it did not account for adhesion effects and debris generation. To increase correlation and avoid discontinuities in the projected results of simulations, the authors suggested that adhesion effects and debris generation be included in the model design.

Odabas [2] conducted a thorough investigation into the effects of sliding speed and normal load on the wear rate of two-body abrasive wear on meticulously prepared samples of 2014 Al Alloy that had been solution treated in a muffle furnace. Wear tests were conducted under dry friction conditions at a sliding distance of 11 m, a speed of 0.36 $ms^{-1}$, a duration of 30 s, and loads in the range of 3-11 $N$ using 220 grit abrasive paper. These tests were conducted to better understand the variation in wear behavior with load and speed.

Odabas [2] discovered that wear rate and load were nearly proportionate up to a critical load of 7 $N$. The slope of the curves decreases after this load due to significant deformation of the worn surface and growing instability of the abrasive grains. When the load on the abrasive grains reaches a critical amount, they begin to shatter. The groove width is approximately 0.17 of the abrasive grain diameter. While the number of contact points increases linearly with load, the relative constant of the groove widths is maintained.

Additionally, Odabas [2] pointed out that the wear volume might be directly proportionate to the applied load if grit wear can be eliminated.

This author's observation regarding single-phase material validates our suggested approach of data interpretation for single-phase alloys using a linear trend line. Similar results were obtained using 150 grit size abrasive materials with a load of 5 *N*, a speed range of 0.09-0.90 *m/s*, and an average sliding distance of 11 *m*.

Kiran et al. [4] studied Wear behavior was evaluated on stir-cast composite samples reinforced with SiCp and Gr particles and manufactured using zinc alloy as the matrix using a pin-on-disc device. Using means and analysis of variance, the effects of the applied load, sliding speed, and sliding distance on wear behavior were investigated. The Taguchi technique was then employed to estimate the parameters that significantly affected wear. A linear regression equation was used to find the correlation between the parameters for each response. The authors noted that the sliding speed and applied load had an effect on the wear volume loss, indicating that increasing any of these parameters will increase the volume loss. Conversely, sliding distance exhibits a negative effect due to the presence of reinforcements in composites.

Amaren et al. [5] used the periwinkle shell sizes of +125µm, +250µm,+335µm,+550µm and 710µm, were mixed with 35wt% of phenolic resin. The periwinkle shell particles were homogeneously mixed and transferred to a mould to produce samples of 20mm diameter and 40mm height. The pin on disc instrument was used to test the dry sliding wear characteristics of the samples. Wear tests were carried out at constant sliding distances of 5000 m, with loads ranging from 40 to 120 kg and sliding speeds of 0.8 to 2.4 m/s at 150 and 250 degrees Celsius. Authors observed that particle sizes of reinforcement (filler) does effect the wear behavior of composite and reported that 125 microns sized periwinkle reinforced composite shown best wear resistance.

From the perspective of the current investigation, it is evident from their published data that as reinforced particle size increases the composites Data on wear loss versus load shows a shift from linear to non-linearity. Smaller reinforced particles function as a single phase material, but larger particle composites exhibit a power law trend line.

Agarwal et al. [6] Prepared composites using chopped E-glass fiber (5-10mm long) as fiber reinforcement, silicon carbide (SiC) of particle size 25-60µm (density 2.6 g/cm$^3$) as filler, epoxy resin of grade LY 556 as matrix material. Composites were prepared by blending epoxy resin, glass fiber and SiC filler in five different weight percent (0 wt% to 20 wt%) with an increment of 5wt% were added with a constant 20wt% of chopped glass fiber. The specimen of size 76mmx 25mmx8mm were prepared. Wear test as per ASTM G65 standard three body abrasion wear tests were conducted by using Tr-50 Dry Abrasion Tester.

According to the authors, the addition of SiC filler causes the Void fraction to slightly drop, hence increasing the composite's strength. It was also mentioned that the specific wear rate of SiC-filled glass fiber reinforced epoxy composites is lower than that of unfilled composites. This is because the specific wear rate of composites is lowered by the interaction between the fiber and filler as well as the uniform dispersion of filler material throughout the composite. Suppressing the particular wear rate of the composite by adding SiC filler beyond 10wt% might not have a major impact.

Pul [9] fabricated the Al 2024-based ZrO2 - reinforced composite materials of sized ≤ 105 µm by vacuum infiltration technique, with ZrO2 with ratios of 5% to 20%) with an increment of 5% as the reinforcing element. The composites materials were prepared to sample size 20mm diameter and 60 mm length. Wear test carried on pin-on-disc instrument with grain- sized abrasive of 280 mesh, 600mesh and 1200mesh. The test conducted under 10N, 20N and 40N load with sliding speed of 0.5 m/s and distance 40m. As the load increases, the wear loss increases for all abrasive size. The wear rate decreases as the $ZrO_2$ % increases for all abrasive size. The highest wear loss was with 280 mesh abrasive $Al_2O_3$. The data was interpreted by optical microscope and scanning electron microscope, and the wetting between Al2024 and $ZrO_2$ was successful. The addition of $ZrO_2$ decreased the wear loss and improved mechanical properties.

Pul [9] observed that the wear resistant behavior of the composite material could be influenced by the size and quantity of the matrix phase as well as the reinforcing elements in the composite structure. This finding confirms our hypothesis, which under certain wear test settings may be used to evaluate wear volume loss vs. load data using a linear and power trend line.

In order to create materials that are resource-efficient, Monikandan et al. [10] created hybrid composites with self-lubricating properties. The mechanical and tribological properties of AA6061-10 weight percent B4C–MoS2 hybrid composites reinforced with 2.5, 5 and 7.5 weight percent concentration of MoS2 particles are assessed on polished samples made using 400, 600, and 1000 grit abrasive sheets. These composites are created using the stir casting technique. A pin-on disc type tribotester (Ducom, TR-20 LE) was used to conduct the dry sliding wear tests. The sliding speeds of 0.5, 1, 1.5, 2, and 2.5 m/s, the applied load of 20 N, and the sliding distance of 1000 m were tested in accordance with ASTM G99-05(2010) standard under atmospheric conditions (1 atm. and 30 ± 1 °C). An 8 mm diameter and 30 mm height cylindrical pin served as the test specimen.

Up to a sliding speed of 2 m/s, the formation of a MoS2-lubricated tribolayer is reported by Monikandan et al. to minimize the wear rate of hybrid composites. Beyond this point, wear rate increases as a result of the MoS2-lubricated tribolayer disintegrating.

The wear behaviour of gravity cast A357 enhanced with dual-size silicon carbide particles was reported by Avinash et al. [11] in 2010. Mould die casting, also known as stir casting, was used to create A357 (Al-7% Sic) alloy reinforced with bimodal sizes of 250µm Large and 38µm Small of 6% Sicp. Three distinct combinations were possible. 4% Big + 2% Small, 3% Big + 3% Small, and 2% Big + 4% Small. The pin-on-disc instrument was tested at a speed of 1 m/s and a load range of 10 to 30 N with 5-N intervals on an EN-32 steel disc. According to the published data, the combination of tiny bimodal distribution (4% large + 2% small) produced the highest levels of hardness and wear resistance. Additionally, they found that wear resistance is greatly impacted by larger concentrations of large-sized particles.

We aimed to demonstrate in this study that comparable conclusions may be reached by comparing their findings with analytical models and interpreting those using power and linear trend lines.

## 3. WEAR MODEL EQUATIONS

Analytical models for wear data interpretation in literature:

### 3.1 Archard model [12]

Archard derived a mathematical model for adhesive wear that has been found to be in good agreement with experimental observations. Equation (1) has been used extensively in describing adhesive wear behaviour.

$$V=\frac{K}{3H}PD \quad (1)$$

Where D is the sliding distance, $P$ is the normal load pressing the two surfaces together,

$H$ is the penetration hardness of the softer material and $K$ is the probability that the rupture of any given junction will result in adhesive wear.

### 3.2 Abrasive wear equation model [12]

From a practical standpoint, the equation for abrasive wear is often written as:

$$V= k\frac{P}{H}D \quad (2)$$

Where K is a combined factor taking into account sharpness, probability of wear and nature of the wear process. $H$ *is* the indentation hardness of the softer material; $P$ is the total load and $D$ is the sliding distance.

### 3.3 Kato model [12]

Kato developed a new parameter wear rate of ceramic materials in lubricated rolling contact.

$$S_C = P_m \frac{\sqrt{Rmax}}{K_{IC}} \quad (3)$$

Sc gives the microscopic and geometrical information of the wear surface.

$K_{IC}$ is the fracture toughness,

$Rmax$ is the maximum surface roughness,

$P_m$ is the mean Hertzian Pressure.

$W=\alpha \cdot Sc^n$

where $\alpha = 1.56\times10^{-5}$ and n=5.46

### 3.4 Evans, Wilshaw & Marshall model [12]

Evans, Wilshaw and Marshall model is a power law equation used for estimating for lateral crack extensions in ceramics.

$$V = C\ \frac{p^{9/8}}{K_{IC}^{1/2}\ H^{5/8}}\left(\frac{E}{H}\right)^{4/5}\ D \tag{4}$$

Where $P$ is the load in N

$D$ is the Sliding Distance in m

$K_{IC}$ fracture toughness

$H$ is the Hardness

where $C$ is a material-independent constant and

$E$ is the elastic modulus.

### Stocia equations [8]

The model equation is given by Stoica et al. for brake pad.

$$v_{u12}=k_{u12}\left(\frac{P}{H}\right)^{\alpha}\ .\left(\frac{v}{v_{cr}}\right)^{\beta}\ =\ k_{u12}\,P_a^{\alpha}\cdot v_a^{\beta} \tag{5}$$

Where $k_{u12}$ are the wear coefficient of pin and disc

$P$ is contact pressure, $H$ is the hardness of disc

$v$ is the sliding speed, $Vcr$ is the critical speed

$P_a = \frac{P}{H}$

$v_a = \frac{v}{v_{cr}}$

$v_{u1}$= volume worn from pad

$v_{u2}$= volume worn from disc

$\alpha$ and $\beta$ are coefficient which depends on material properties, friction, temperature etc, (in many situations $\alpha = \beta \approx 1$).

$p.v$ is a parameter of the energy flux.

### Wear measurements:

$$\text{Wear loss } \Delta w = (w_1 - w_2) \text{ in g} \tag{6}$$

$$\text{Volume loss} = \frac{(w_1 - w_2)}{\rho} \tag{7}$$

$$\text{Volume loss(V) mm}^3 = \frac{mass\ loss}{Density\ g/mm^3} X1000 \tag{8}$$

$$\text{Wear rate (g/m)} = \frac{mass\ loss\ (g)}{Sliding\ distance\ (m)} \tag{9}$$

$$\text{Specific Wear rate } (W_s)\ = \frac{V\ m^3}{F(N)\times S(m)} \tag{10}$$

Where '$S$' is sliding distance $S = v \times t$

where t is time duration in seconds and v is speed.

## 4. INTERPRETATION METHOD

### 4.1 X-Y Extract

Pin-on-disc experimental wear data from published research papers is measured using X-Y extract software and graph readings are converted in our required format and drawn the graph wear loss vs load.

### 4.2 Linear trend line fitting (Archard, abrasive)

From Archard equation

$$V=\frac{K}{3H}PD$$

$$V=[\frac{K\ D}{3H}]\ P$$

For a given material $\frac{K}{3H}$ is a material constant and $P$ *(load)* for the testing condition, above equation may be compared with a straight line as expressed below:

$$Y = a*X$$

*Here,* $a$ is the slope of the line X-$Y$, when compared with Archard equation we can write,

$$a=\frac{KD}{3H}$$

$a$ is the experimental constant.

As the hardness of the material increases the slope $a$ of linear curve reduces and thus wear decreases.

### 4.3 Power trend line fitting

From Evans, Wilshaw & Marshall model equation

$$V = C\ \frac{P^{9/8}}{K_{IC}^{1/2}\ H^{5/8}}\left(\frac{E}{H}\right)^{4/5}\ D$$

When compared above equation with two parameter power equation

$$V = a\ P^b$$

Here, $P$ is the load applied and $a$ may befied as below:

$$a = C\ \frac{1}{K_{IC}^{1/2}\ H^{5/8}}\left(\frac{E}{H}\right)^{4/5}\ D$$

For a given sample Young's modulus ($E$), Hardness ($H$), and Fracture Toughness ($K_{IC}$) is constant, and then Wear volume loss ($V$) is defined as below:

$$V\ \alpha\ P^b$$

Here, $a$ and $b$ is dependent upon both experimental characteristics like hardness of disc and pin, lubrication etc and material characteristics like homogeneity, toughness hardness etc.

In above equation if $b$= 1, then it becomes linear wear equation, here wear obeys the Abrasive model equation without any interference of other experimental conditions like crack arrest, lubrication effect etc.

If $b \neq 1$, it becomes a power law wear equation, here crack propagation may be arrested during wear or due to formation wear debris lubrication may be effected etc.

If the modulus, hardness and toughness of the materials is determined by experiments one can define physical meaning of parameters $a$ and $b$.

In this study, experimental wear data from literature [2,6,9] for various conditions, are interpreted by in built linear and power trend-line using Excel spreadsheet program to determine $a$ and $b$.

## 5. VALIDATION OF PUBLISHED EXPERIMENTAL DATA WITH PUBLISHED WEAR MODEL EQUATION

Odabas reported in the paper Effects of Load and Speed on Wear Rate of Abrasive Wear for 2014 Al Alloy [2].

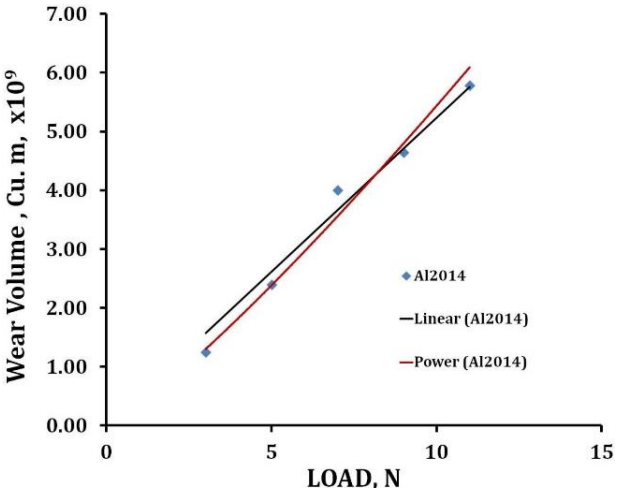


**Fig. 1.** Shows wear loss values of Al 2014 [2].

**Table 1.** Shows the graphical data of Linear trend line is summarized in table of Abrasive wear for 2014 Al Alloy.

| Data obtained from Linear trendline fit | | |
|---|---|---|
| **Plot** | **Slope ($a$)** | **R-Square** |
| WEAR LOSS | $5.0\times10^{-10}$ | 0.9965 |

**Table 2.** Shows the graphical data of Power trend line is summarized in table of Abrasive wear for 2014 Al Alloy.

| Data obtained from Power trendline fit | | | |
|---|---|---|---|
| **Plot** | ***a*** | ***b*** | **R-Square** |
| WEAR LOSS | $4.0\times10^{-10}$ | 1.189 | 0.9798 |

It is pure Al alloy material of single phase homogenous in nature, crack may propagate in a same manner. Therefore, it is following Abrasive nature.

Agarwal et al. [6] reported in paper,

Composites were fabricated by blending epoxy resin, glass fiber and SiC filler reinforced With fixed wt.% of chopped glass fiber reinforcement.

SiC filler in wt percent 0%,5%,10%,15% and 20%

- Addition of SiC reduces the wear rate significantly SiC acts as filler and reduces the porosity to 0%
- Microcracking and Micro ploughing are dominate wear mechanism observed as also interpreted by our method.
- In our study it is observed the same by interpretation of authors data by trendline and comparing it with analytical models.

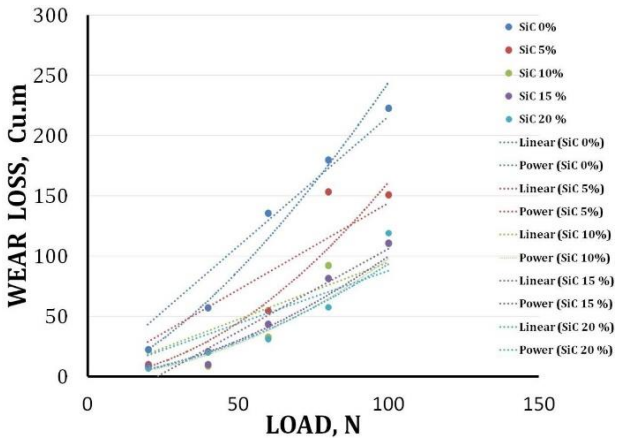


**Fig. 2.** Shows wear loss values of SiC-filled glass fibre-reinforced epoxy composite [6].

**Table 3**. Shows the graphical data of Linear trend is summarized in table for SiC filled glass fibre reinforced epoxy composite.

| Data obtained from Linear trendline fit | | |
|---|---|---|
| **SiC %** | **Slope** *(a)* | **R-Square** |
| 0% | 2.1601 | 0.9864 |
| 5% | 1.4389 | 0.9151 |
| 10% | 0.9492 | 0.9049 |
| 15% | 0.9455 | 0.8325 |
| 20% | 0.8768 | 0.8962 |

**Table 4**. Shows the graphical data of Power trend line is summarized in table for SiC filled glass fibre reinforced epoxy composite.

| Data obtained from Power trend line fit | | | |
|---|---|---|---|
| **SiC %** | ***a*** | ***b*** | **R-Square** |
| 0% | 0.2678 | 1.4801 | 0.9711 |
| 5% | 0.031 | 1.8541 | 0.8824 |
| 10% | 0.0203 | 1.841 | 0.9434 |
| 15% | 0.0334 | 1.7384 | 0.9795 |
| 20% | 0.0362 | 1.7061 | 0.9413 |

Interpretation by Trend Line

- At 0% SiC void spaces are more, therefore crack nucleate and propagate.
- When SiC is added it may occupies void spaces in GFRE( Glass fiber reinforced epoxy) and prevent the crack propagation and therefore power trendline fits more than linear trendline.
- Two mechanisms of wear loss are proposed by authors based on SEM studies carried out by them (1) crack propagation and (2) ploughing (Abrasive wear).
- In 5% SiC wear loss may be attributed to crack propagation, when compared with ploughing (abrasive wear), power trend is more likely to fit the data points.
- In 15% SiC by trend analysis, it is observed that wear loss, from volume loss vs load data, obtained under controlled experimental conditions.

At 0% SiC however $b \neq 1$ because epoxy present in specimen.

As the content of SiC increases $R^2$ of linear trendline less than $R^2$ of power trendline it obeys the power law equation, here the crack propagation are attrested.

Pul [9] reported in the paper Effect of $ZrO_2$ quantity on mechanical properties of $ZrO_2$ - reinforced aluminum composites produced by the vacuum infiltration technique**.**

SAMPLES: $ZrO_2$ - Reinforced Aluminum composites
$ZrO_2$ in the range 5%,10%,15%,20%
Size ≤105μ
Wetting between Al2024 and $ZrO_2$ is successful
Wear test carried for the specimen
280 mesh (52 μm)
600 mesh (19 μm)
1200 mesh (12 μm) grain sized abrasives
Normal load 10N, 20N, and 40N.
Sliding speed 0.5 m/s
Sliding distance 40m

The wear losses obtained from pin-on-disc instrument for Al2024 composites reinforced with 5%,10%,15% and 20% of $ZrO_2$ and drawn graph wear loss versus $ZrO_2$ ratio % wt, these graph readings are converted in our required format with help of X-Y extract software and drawn the graph wear loss vs load.

The curve is fitted with linear trend line and power trend line for graph Wear loss values of $ZrO_2$-reinforced Al 2024 composites for 280, 600 and 1200 Abrasive paper as shown in graph Fig 3,4 and 5 respectively. The graphical data of Linear trend line summarized for $ZrO_2$-reinforced Al 2024 composites for all Abrasive paper in tables.

The wear losses decrease with the increase in $ZrO_2$ reinforcement ratio in composite. The highest wear loss at 40N. The highest wear loss for 280 mesh abrasive.

At 0% $ZrO_2$ is a brittle fracture, crack propagation is uniformly distributed.

At 5% $ZrO_2$, Crack propagation is not uniformly distributed.

An increase in the $ZrO_2$ reinforcement ratio cause agglomeration (at 15% $ZrO_2$).

The results are shown in graph wear loss vs % load for all ratios of $ZrO_2$ -reinforced Al2024 composites.

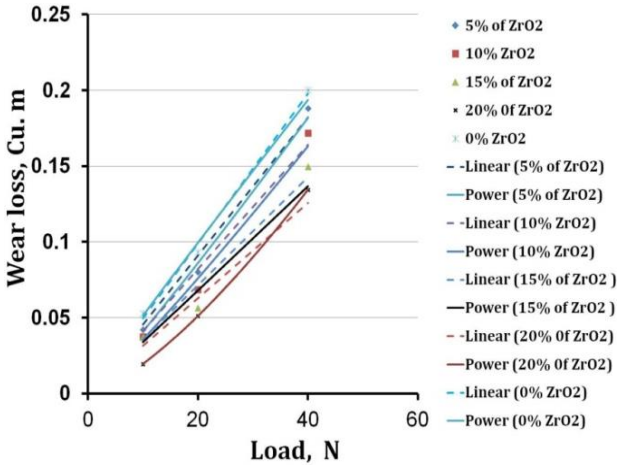


**Fig. 3.** Shows Wear loss values of $ZrO_2$-reinforced Al 2024 composites for 280 Abrasive paper [9].

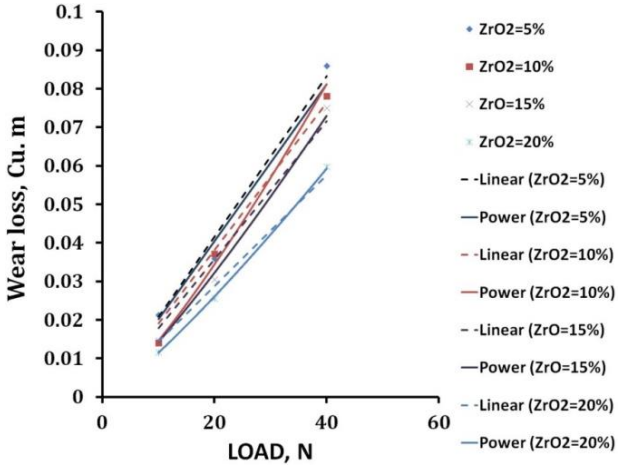


**Fig. 4.** Shows Wear loss values of $ZrO_2$-reinforced Al 2024 composites for 600 Abrasive paper [9].

**Table 5.** Shows the graphical data of Linear trend line summarized for $ZrO_2$-reinforced Al 2024 composites for 280 Abrasive paper.

| Data obtained from Linear trendline fit | | |
|---|---|---|
| **$ZrO_2$ %** | **Slope(*a*)** | **R-Square** |
| 0% | 0.0049 | 0.999 |
| 5% | 0.0045 | 0.9962 |
| 10% | 0.0041 | 0.9927 |
| 15% | 0.0036 | 0.9901 |
| 20% | 0.0031 | 0.9829 |

**Table 6.** Shows the graphical data of Power trend line summarized for $ZrO_2$-reinforced Al 2024 composites for 280 Abrasive paper.

| Data obtained from Power trendline fit | | | |
|---|---|---|---|
| **$ZrO_2$%** | ***a*** | ***b*** | **R-Square** |
| 0% | 0.0056 | 0.9597 | 0.9947 |
| 5% | 0.0034 | 1.0779 | 0.9955 |
| 10% | 0.0028 | 1.1009 | 0.9911 |
| 15% | 0.0033 | 1.007 | 0.9716 |
| 20% | 0.0008 | 1.3929 | 1 |

From linear tread $R^2$ is reduced from 0% to 20% $ZrO_2$.

At 0% $ZrO_2$ as comparing $R^2$ of linear tread line and power tread line, linear tread line increases, it obeys the linear tread line.

At 5% $ZrO_2$ because few particles of $ZrO_2$ of 280 mesh (52 micron) here obeys both the law.

At 10% $ZrO_2$ ,from table 6, $b$=1.10, more than 1, it obeys the power law equation model.

At 20% $ZrO_2$, $R^2$=1 and $b$=1.3929, it obeys the power law equation model.

**Table 7.** Shows the graphical data of Linear trend line is summarized in table for $ZrO_2$-reinforced Al 2024 composites for 600 Abrasive paper.

| ≈Data obtained from Linear trendline fit | | |
|---|---|---|
| **$ZrO_2$ %** | **Slope(*a*)** | **R-Square** |
| 5% | 0.0021 | 0.9957 |
| 10% | 0.0019 | 0.9962 |
| 15% | 0.0018 | 0.9925 |
| 20% | 0.0014 | 0.9948 |

**Table 8.** Shows the graphical data of Power trend line is summarized in table for $ZrO_2$-reinforced Al 2024 composites for 600 Abrasive paper.

| Data obtained from Power trendline fit | | | |
|---|---|---|---|
| **$ZrO_2$ %** | ***a*** | ***b*** | **R-Square** |
| 5% | 0.002 | 1.0051 | 0.9868 |
| 10% | 0.0008 | 1.2382 | 0.9949 |
| 15% | 0.0009 | 1.1788 | 0.9977 |
| 20% | 0.0008 | 1.1834 | 0.9997 |

The analaysis of graphical data from table 7 and table 8. for $ZrO_2$ for 600 abrasive paper, results from this study can be summariezed as:

- At 5% $ZrO_2$ $R^2$ value of linear trend line and power trend line are comparable. Therefore it can be interpreted that 5% $ZrO_2$ wear behaviour follows linear trend of volume loss vs force. However, higher amount of $ZrO_2$ follows power trend line suggesting that hardenss effect is significant. If we refer authors Brinnel hardness data, it can be observed at 5%
- At 10% $ZrO_2$ $b$=1.238 it obeys the power law equation.
- At 15% $ZrO_2$ $b$=1.178 it obeys the power law equation.
- At 20% $ZrO_2$ $b$=1.18 it obeys the power law equation.

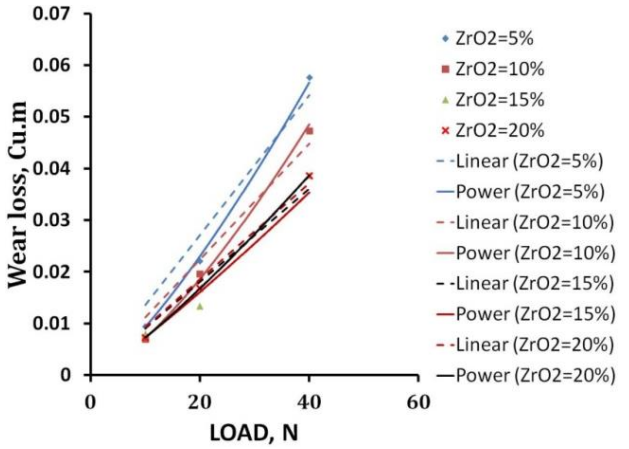


**Fig. 5.** Shows Wear loss values of $ZrO_2$-reinforced Al 2024 composites for 1200 Abrasive paper [9].

**Table 9.** Shows the graphical data is summarized in table for $ZrO_2$-reinforced Al 2024 composites for 1200 Abrasive paper.

| Data obtained from Linear trendline fit | | |
|---|---|---|
| **$ZrO_2$ %** | **Slope (*a*)** | **R-Square** |
| 5% | 0.0014 | 0.9864 |
| 10% | 0.0011 | 0.9878 |
| 15% | 0.0009 | 0.9831 |
| 20% | 0.0009 | 0.995 |

**Table 10.** Shows the graphical data is summarized in table for $ZrO_2$-reinforced Al 2024 composites for 1200 Abrasive paper.

| Data obtained from Power trendline fit | | | |
|---|---|---|---|
| **$ZrO_2$ %** | ***a*** | ***b*** | **R-Square** |
| 5% | 0.0005 | 1.3021 | 0.9992 |
| 10% | 0.0003 | 1.3856 | 0.9984 |
| 15% | 0.0005 | 1.1389 | 0.9794 |
| 20% | 0.00045 | 1.2083 | 1 |

The analaysis of graphical data from table 9 and table 10, for $ZrO_2$ for 1200 abrasive paper.

For all percentages of $ZrO_2$, comparing slope, ***a***, it can observed that slope decreases with inclrease percentage of $ZrO_2$ suggesting that, wear loss decrease with increase in amount of $ZrO_2$. In case of power trendline fit, one can observe that at around 15 % , data approximately agrees with Evans-Wilshaw and Marshall (EVM) model equation, suggesting that toughness, hardness, and elastic modulus are affecting the wearloss and material is homogenous. Further, As $ZrO_2$ increase beyond 15 %, the parameters are not camparable with the EVM model suggesting that in-homogeniety in the material due to agglomeration or so.

The $R^2$ value of linear trend line and power trend line, power trend line goodness of fit is greater than linear trend line goodness of fit. For example, at 20% $ZrO_2$ $R^2$ (0.99) is lower than 5% $ZrO_2$ for trendline ($R^2$=1).

At 5% $ZrO_2$ $b$=1.30, it obeys the power trend line. At 10% $ZrO_2$ $b$=1.38 and at 15% $ZrO_2$ $b$=1.13 it obeys the power law equation, as the author reported at 15% $ZrO_2$ the reinforcement ratio causes agglomerations, the same observations from trend line technique. For 20% $ZrO_2$ the power law of $R^2$=1 and $b$=1.20.

For all ratios % of $ZrO_2$ fits the power law because of fine abrasive paper of 12 micron. Here crack propagation are attrested and it is goodness of fit.

The published pin-on-disc experimental data with information from SEM or XRD of two-phase material Al 2024 and $ZrO_2$-reinforced aluminum composites and multiphase material SiC filled chopped glass fiber reinforced epoxy.

Composites are interpreted by analytical model with trend line technique and observed that our results are similar to author observations.

## 6. CONCLUSION

- In general, it is observed in reported literature that wear data is interpreted by experiment methods with SEM (Microscopic techniques) which is time consuming and expensive.
- In this study an attempt is made to interpret wear data by analytical models and observed that conclusions drawn from this method are similar to authors' observations from the same data from various papers.
- To summarize this trend line technique which is more economical and this technique can also be extended to routine quality checks in Industry.
- In future, systematic experiments would be conducted to generate wear data for validation of this technique.

## REFERENCES


[1] E. M. Bortoleto *et al.*, "Experimental and numerical analysis of dry contact in the pin on disc test," *Wear*, vol. 301, no. 1–2, pp. 19–26, Apr. 2013, doi: 10.1016/j.wear.2012.12.005.

[2] D. Odabaş, "Effects of load and speed on wear rate of abrasive wear for 2014 Al Alloy," *IOP Conference Series: Materials Science and Engineering*, vol. 295, p. 012008, Jan. 2018, doi: 10.1088/1757-899x/295/1/012008.

[3] A. O. Rajole, S. V Gubbewad, and A. R. Raichur, "Wear Behaviour of PLA, ABS and Alumina Filled PLA Composite: A Comparative Study," *International Journal of Science and Research (IJSR)*, vol. 11, no. 6, pp. 1519-1523, Jun. 20122. doi: 10.21275/SR22622133914.

[4] T. Kiran, M. Kumar, S. Basavarajappa, and B. M. Viswanatha, "Dry sliding wear behavior of heat treated hybrid metal matrix composite using Taguchi techniques," *Materials in Engineering*, vol. 63, pp. 294–304, Nov. 2014, doi: 10.1016/j.matdes.2014.06.007.

[5] S. G. Amaren, D. S. Yawas, and S. Y. Aku, "Effect of periwinkles shell particle size on the wear behavior of asbestos free brake pad," *Results in Physics*, vol. 3, pp. 109–114, Jan. 2013, doi: 10.1016/j.rinp.2013.06.004.

[6] G. Agarwal, A. Patnaik, and R. K. Sharma, "Parametric optimization and three-body abrasive wear behavior of sic filled chopped glass fiber reinforced epoxy composites," *International Journal of Composite Materials*, vol. 3, no. 2, pp. 32–38, Jan. 2013, doi: 10.5923/j.cmaterials.20130302.02.

[7] V. L. Popov, "Generalized archard law of wear based on rabinowicz criterion of wear particle formation," *Facta Universitatis*, vol. 17, no. 1, p. 39, Mar. 2019, doi: 10.22190/fume190112007p.

[8] S. Alexandru, P. Alina-Maria, and A. Tudor, "Modelling the wear processes of the automotive brake pad and disc," *INCAS Buletin*, vol. 10, no. 4, pp. 169–179, Dec. 2018, doi: 10.13111/2066-8201.2018.10.4.15.

[9] M. Pul, "Efecto de la cantidad de $ZrO_2$ sobre las propiedades mecánicas de los compuestos de aluminio reforzados con $ZrO_2$ producidos por la técnica de infiltración al vacío," *Revista De Metalurgia*, vol. 57, no. 2, p. e195, Jun. 2021, doi: 10.3989/revmetalm.195.

[10] V. V. Monikandan, M. A. Joseph, and P. K. Rajendrakumar, "Dry sliding wear studies of aluminum matrix hybrid composites," *Resource-Efficient Technologies*, vol. 2, pp. S12–S24, Dec. 2016, doi: 10.1016/j.reffit.2016.10.002.

[11] L. Avinash, T. R. Prabhu, and S. Bontha, "The Effect on the Dry Sliding Wear Behavior of Gravity Cast A357 Reinforced with Dual Size Silicon Carbide Particles," *Applied Mechanics and Materials*, vol. 829, pp. 83–89, Mar. 2016, doi: 10.4028/www.scientific.net/amm.829.83.

[12] F. M. Huq, *Development of life prediction models for rolling contact wear in ceramic and steel ball bearings*, RMIT University: Masters by Research, Melbourne, 2007.